Supporting Information

Highly Active and Selective Electrocatalytic CO_2 Conversion Enabled by Core/Shell Ag/(Amorphous-Sn(IV)) Nanostructures with Tunable Shell Thickness

Jin Zhang,[†,=] Man Qiao,[#,=] Yafei Li,[#,*] Qi Shao[†,*] and Xiaoqing Huang[†,*]

[†]College of Chemistry, Chemical Engineering and Materials Science, Soochow University, Jiangsu, 215123, China.

[#]Jiangsu Collaborative Innovation Centre of Biomedical Functional Materials, School of Chemistry and Materials Science, Nanjing Normal University, Nanjing, 210023, China.

[=]These authors contribute equally.

*Address correspondence to: liyafei@njnu.edu.cn; qshao@suda.edu.cn; hxq006@suda.edu.cn

Computational Method: In this work, the SnO_2 (110) surface is adopted to simulate A-Sn(IV) shell as shown in Supplementary Figure S27. Based on experimentally measured thickness (0.51 nm to 0.94 nm), we employed 6 (0.6nm) and 9 (0.9nm) atomic layers thickness to calculate free energy profiles. The thinnest two A-Sn(IV) shell consist of only 6 and 9 atomic layers, due to the presence of the substrate and periodicity. Moreover, the Ag/A-Sn(IV) shell is model by replacing one surface Sn atom with one Ag atom. DFT computations were performed using the plane-wave technique implemented in Vienna *ab initio* simulation package (VASP). The ion-electron interaction was described using the projector-augmented plane wave (PAW) approach. The generalized gradient approximation (GGA) expressed by PBE functional and a 420 eV cutoff for the plane-wave basis set were adopted in all the computations. The Gaussian smearing method with σ value 0.1 eV was used in this system. The convergence threshold was set as 10^{-5} eV in energy and 0.04 eV/Å in force. A Monkhorst−Pack grid 5×5×1 was chosen for slab calculation. The vacuum was chosen 15 Å to avoid images interactions. The solvent effect on adsorbates was simulated using the Poissson-Boltzmann implicit solavtion model with a dielectric constant of 80. For the SnO_2 and Ag/SnO_2 shell, the top three atomic layers were relaxed while the other layers were fixed at the bulk lattice position.

The computational hydrogen electrode (CHE) method has been applied to determine the Gibbs free energy of reaction intermediates. In this method, the electrochemical potential of an electron-proton pair (H^++e^-) is equal to the free energy of half of hydrogen (1/2H_2) at standard pressure. The ECR involve 2e pathway can be classified into two types:

$$CO_2\,(g) + (H^+ + e^-) + * \rightarrow OCHO^*$$

$$OCHO^* + (H^+ + e^-) \rightarrow * + HCOOH\,(l) \qquad (1)$$

$$CO_2\,(g) + (H^+ + e^-) + * \rightarrow COOH^*$$

$$COOH^* + (H^+ + e^-) \rightarrow CO^* + H_2O \rightarrow * + CO\,(g) \qquad (2)$$

Where * represents the adsorption site, OCHO*, COOH* and CO* represent reaction intermediates, respectively. The free energy (G) of each species is estimated at T=298 K according to:

$$G = E_{DFT} + E_{ZPE} - TS$$

where E_{DFT}, E_{ZPE} and S, is electronic energy, zero point energy, entropy, respectively. For adsorbed intermediates, E_{ZPE} and S were determined by vibration frequencies calculations, where all 3N degrees of freedom are treated as harmonic vibration motions with neglecting contributions from the slab, while for molecules those were taken from the NIST database. The contribution of zero point energy and entropy corrections to G is provided in **Table S2**.

Note. Detailed information of structures for calculation.

SnO_2-sur:

```
1.00000000000000
   6.5065999030999997   0.0000000000000000   0.0000000000000000
   0.0000000000000000   6.8080000877000000   0.0000000000000000
   0.0000000000000000   0.0000000000000000  24.4421997070000003
  Sn   O
  8   16
Selective dynamics
```

Direct

0.1269399970000009	0.1786199960000019	0.2258799969999998	F	F	F
0.6269400119999986	0.1786199960000019	0.2258799969999998	F	F	F
0.1269399970000009	0.6787042607098644	0.3626333061033261	T	T	T
0.6269400119999986	0.6787042607098644	0.3626333061033261	T	T	T
0.3769400119999986	0.6786199809999971	0.2258799969999998	F	F	F
0.8769400119999986	0.6786199809999971	0.2258799969999998	F	F	F
0.3769400119999986	0.1786744423594480	0.3703012067086885	T	T	T
0.8769400119999986	0.1786744423594480	0.3703012067086885	T	T	T
0.1269399970000009	0.6786199809999971	0.1720000059999975	F	F	F
0.6269400119999986	0.6786199809999971	0.1720000059999975	F	F	F
0.1269399970000009	0.1787857734081463	0.3112813278959974	T	T	T
0.6269400119999986	0.1787857734081463	0.3112813278959974	T	T	T
0.1269399970000009	0.6786199809999971	0.2797699870000017	F	F	F
0.6269400119999986	0.6786199809999971	0.2797699870000017	F	F	F
0.1269399970000009	0.1786447844876365	0.4203185346949261	T	T	T
0.6269400119999986	0.1786447844876365	0.4203185346949261	T	T	T
0.3769400119999986	0.3720799979999967	0.2258799969999998	F	F	F
0.8769400119999986	0.3720799979999967	0.2258799969999998	F	F	F
0.3769400119999986	0.8650198314414456	0.3726974586810338	T	T	T
0.8769400119999986	0.8650198314414456	0.3726974586810338	T	T	T
0.3769400119999986	0.9851499800000028	0.2258799969999998	F	F	F
0.8769400119999986	0.9851499800000028	0.2258799969999998	F	F	F
0.3769400119999986	0.4923148893198179	0.3726691541314943	T	T	T
0.8769400119999986	0.4923148893198179	0.3726691541314943	T	T	T

SnO_2-COOH:

1.00000000000000

6.5065999030999997	0.0000000000000000	0.0000000000000000
0.0000000000000000	6.8080000877000000	0.0000000000000000
0.0000000000000000	0.0000000000000000	24.4421997070000003

Sn	O	C	H
8	18	1	1

Selective dynamics

Direct

0.1269399970000009	0.1786199960000019	0.2258799969999998	F	F	F
0.6269400119999986	0.1786199960000019	0.2258799969999998	F	F	F
0.1270058644478368	0.6794760899412299	0.3616079301162096	T	T	T
0.6271779468483299	0.6809876799905863	0.3660427049718638	T	T	T
0.3769400119999986	0.6786199809999971	0.2258799969999998	F	F	F
0.8769400119999986	0.6786199809999971	0.2258799969999998	F	F	F
0.3766878347714309	0.1801150323145815	0.3691453914360028	T	T	T
0.8780078721363714	0.1799414738724031	0.3691855156822218	T	T	T
0.1269399970000009	0.6786199809999971	0.1720000059999975	F	F	F
0.6269400119999986	0.6786199809999971	0.1720000059999975	F	F	F
0.1271828405233598	0.1813895243978477	0.3105546190087086	T	T	T
0.6273284079442816	0.1803330581842832	0.3107681902756619	T	T	T
0.1269399970000009	0.6786199809999971	0.2797699870000017	F	F	F
0.6269400119999986	0.6786199809999971	0.2797699870000017	F	F	F
0.1273900627381638	0.1797682430120073	0.4200889677198451	T	T	T
0.6272297998363510	0.1779687690493317	0.4195340343339433	T	T	T
0.3769400119999986	0.3720799979999967	0.2258799969999998	F	F	F
0.8769400119999986	0.3720799979999967	0.2258799969999998	F	F	F
0.3711605271428426	0.8697361924310184	0.3683980425462876	T	T	T
0.8829394413630173	0.8695910680463065	0.3686834508309927	T	T	T
0.3769400119999986	0.9851499800000028	0.2258799969999998	F	F	F
0.8769400119999986	0.9851499800000028	0.2258799969999998	F	F	F
0.3721588387291970	0.4908721905748449	0.3699004964322935	T	T	T

0.8819917911115416 0.4907848316902480 0.3701801409416560 T T T
0.7851303761783707 0.6927891190110086 0.4890294309367055 T T T
0.4356467332935050 0.6885878355453618 0.4838741702170008 T T T
0.6245295393036564 0.6890587127103747 0.4638166363477028 T T T
0.4384004995708918 0.6924588070528164 0.5244118694376938 T T T

SnO_2-OCHO:
1.00000000000000
6.5065999030999997 0.0000000000000000 0.0000000000000000
0.0000000000000000 6.8080000877000000 0.0000000000000000
0.0000000000000000 0.0000000000000000 24.4421997070000003
Sn O C H
8 18 1 1
Selective dynamics
Direct
0.1269399970000009 0.1786199960000019 0.2258799969999998 F F F
0.6269400119999986 0.1786199960000019 0.2258799969999998 F F F
0.1289651319938005 0.6781294304512034 0.3649011620749822 T T T
0.6240318396307852 0.6781631738941269 0.3649420754876427 T T T
0.3769400119999986 0.6786199809999971 0.2258799969999998 F F F
0.8769400119999986 0.6786199809999971 0.2258799969999998 F F F
0.3769574547059024 0.1784839024616764 0.3669379174180198 T T T
0.8768013172478389 0.1784149865979399 0.3689853664104261 T T T
0.1269399970000009 0.6786199809999971 0.1720000059999975 F F F
0.6269400119999986 0.6786199809999971 0.1720000059999975 F F F
0.1229464021279038 0.1783963390816509 0.3102501475008086 T T T
0.6307054490195227 0.1781662560814275 0.3102207756292549 T T T
0.1269399970000009 0.6786199809999971 0.2797699870000017 F F F
0.6269400119999986 0.6786199809999971 0.2797699870000017 F F F
0.1292151881932765 0.1789516666413874 0.4189667968941723 T T T
0.6243077407063045 0.1788690889995277 0.4189762341315714 T T T
0.3769400119999986 0.3720799979999967 0.2258799969999998 F F F
0.8769400119999986 0.3720799979999967 0.2258799969999998 F F F
0.3766046501647615 0.8722907255042336 0.3619356683933813 T T T
0.8766338443432710 0.8666850722696087 0.3718148016292486 T T T
0.3769400119999986 0.9851499800000028 0.2258799969999998 F F F
0.8769400119999986 0.9851499800000028 0.2258799969999998 F F F
0.3765268591832751 0.4841942813307533 0.3609093116924016 T T T
0.8764611417979192 0.4900684663121077 0.3714514121596585 T T T
0.1979476329528074 0.6731088903399819 0.4527322667411883 T T T
0.5538871953579956 0.6729818232477762 0.4528162161431286 T T T
0.3758860056573659 0.6689272241141427 0.4747024751700900 T T T
0.3756005565541226 0.6600888053683773 0.5197694925275732 T T T

SnO_2-CO:
1.00000000000000
6.5065999030999997 0.0000000000000000 0.0000000000000000
0.0000000000000000 6.8080000877000000 0.0000000000000000
0.0000000000000000 0.0000000000000000 24.4421997070000003
Sn O C
8 17 1
Selective dynamics
Direct
0.1269399970000009 0.1786199960000019 0.2258799969999998 F F F
0.6269400119999986 0.1786199960000019 0.2258799969999998 F F F
0.1277733873541161 0.6800090404923332 0.3622746996428134 T T T
0.6279142539478419 0.6795905702313455 0.3630494855613354 T T T
0.3769400119999986 0.6786199809999971 0.2258799969999998 F F F
0.8769400119999986 0.6786199809999971 0.2258799969999998 F F F

0.3778996287537801 0.1798935186057787 0.3704354223795557 T T T
0.8787395724968451 0.1798727224719486 0.3704298747203975 T T T
0.1269399970000009 0.6786199809999971 0.1720000059999975 F F F
0.6269400119999986 0.6786199809999971 0.1720000059999975 F F F
0.1277259042317904 0.1790950506407725 0.3113034970081583 T T T
0.6277506959451625 0.1791155734799081 0.3114376281332503 T T T
0.1269399970000009 0.6786199809999971 0.2797699870000017 F F F
0.6269400119999986 0.6786199809999971 0.2797699870000017 F F F
0.1283752941158522 0.1801236719515853 0.4206604916949496 T T T
0.6283995672868127 0.1804827018788656 0.4205713251193917 T T T
0.3769400119999986 0.3720799979999967 0.2258799969999998 F F F
0.8769400119999986 0.3720799979999967 0.2258799969999998 F F F
0.3768042696248925 0.8666866271165032 0.3723161522782497 T T T
0.8789496413298563 0.8666567381398403 0.3724060217954119 T T T
0.3769400119999986 0.9851499800000028 0.2258799969999998 F F F
0.8769400119999986 0.9851499800000028 0.2258799969999998 F F F
0.3764427539718059 0.4930561301523320 0.3721965714094594 T T T
0.8792004022213946 0.4930372994247778 0.3722632182466175 T T T
0.6076072749426983 0.6706975363141982 0.5135748759036254 T T T
0.6196559303614171 0.6751117794980286 0.4671633098124107 T T T

SnO_2-H:
1.00000000000000
6.5065999030999997 0.0000000000000000 0.0000000000000000
0.0000000000000000 6.8080000877000000 0.0000000000000000
0.0000000000000000 0.0000000000000000 24.4421997070000003
Sn O H
8 16 1
Selective dynamics
Direct
0.1269399970000009 0.1786199960000019 0.2258799969999998 F F F
0.6269400119999986 0.1786199960000019 0.2258799969999998 F F F
0.1269399970000009 0.6787805164785815 0.3615996908502094 T T T
0.6269400119999986 0.6789163016350965 0.3694195583120981 T T T
0.3769400119999986 0.6786199809999971 0.2258799969999998 F F F
0.8769400119999986 0.6786199809999971 0.2258799969999998 F F F
0.3757189390218275 0.1788788598970957 0.3680315655759672 T T T
0.8781610849781694 0.1788788598970957 0.3680315655759672 T T T
0.1269399970000009 0.6786199809999971 0.1720000059999975 F F F
0.6269400119999986 0.6786199809999971 0.1720000059999975 F F F
0.1269399970000009 0.1791002101752413 0.3100805186551604 T T T
0.6269400119999986 0.1789605352935906 0.3103514784824166 T T T
0.1269399970000009 0.6786199809999971 0.2797699870000017 F F F
0.6269400119999986 0.6786199809999971 0.2797699870000017 F F F
0.1269399970000009 0.1789465856970153 0.4199170528092494 T T T
0.6269400119999986 0.1788241045061777 0.4186673498787824 T T T
0.3769400119999986 0.3720799979999967 0.2258799969999998 F F F
0.8769400119999986 0.3720799979999967 0.2258799969999998 F F F
0.3687235925527084 0.8708983078129515 0.3671190416446785 T T T
0.8851564314472885 0.8708983078129515 0.3671190416446785 T T T
0.3769400119999986 0.9851499800000028 0.2258799969999998 F F F
0.8769400119999986 0.9851499800000028 0.2258799969999998 F F F
0.3687957917005839 0.4868625186188471 0.3672226652374075 T T T
0.8850842322994137 0.4868625186188471 0.3672226652374075 T T T
0.6269400119999986 0.6793660962110598 0.4407087611758229 T T T

Ag-SnO_2-sur:
1.00000000000000

6.5065999030999997 0.0000000000000000 0.0000000000000000
0.0000000000000000 6.8080000877000000 0.0000000000000000
0.0000000000000000 0.0000000000000000 24.4421997070000003
Sn Ag O
7 1 16
Selective dynamics
Direct
0.1269399970000009 0.1786199960000019 0.2258799969999998 F F F
0.6269400119999986 0.1786199960000019 0.2258799969999998 F F F
0.6269400119999986 0.6788431835617152 0.3628209071575058 T T T
0.3769400119999986 0.6786199809999971 0.2258799969999998 F F F
0.8769400119999986 0.6786199809999971 0.2258799969999998 F F F
0.3738481143052503 0.1788130291447643 0.3690676451261198 T T T
0.8800319096947469 0.1788130291447643 0.3690676451261198 T T T
0.1269399970000009 0.6788645783457532 0.3722526746720615 T T T
0.1269399970000009 0.6786199809999971 0.1720000059999975 F F F
0.6269400119999986 0.6786199809999971 0.1720000059999975 F F F
0.1269399970000009 0.1787609922531286 0.3109229153548513 T T T
0.6269400119999986 0.1788227889999276 0.3112042607927975 T T T
0.1269399970000009 0.6786199809999971 0.2797699870000017 F F F
0.6269400119999986 0.6786199809999971 0.2797699870000017 F F F
0.1269399970000009 0.1787096020475659 0.4201434410474517 T T T
0.6269400119999986 0.1786839820427118 0.4194987549707877 T T T
0.3769400119999986 0.3720799979999967 0.2258799969999998 F F F
0.8769400119999986 0.3720799979999967 0.2258799969999998 F F F
0.3803417743926780 0.8656253782770916 0.3757834646131688 T T T
0.8735382496073192 0.8656253782770916 0.3757834646131688 T T T
0.3769400119999986 0.9851499800000028 0.2258799969999998 F F F
0.8769400119999986 0.9851499800000028 0.2258799969999998 F F F
0.3803422467057910 0.4920244357020584 0.3757977359359634 T T T
0.8735377772942065 0.4920244357020584 0.3757977359359634 T T T

Ag-SnO_2-COOH:
1.00000000000000
6.5065999030999997 0.0000000000000000 0.0000000000000000
0.0000000000000000 6.8080000877000000 0.0000000000000000
0.0000000000000000 0.0000000000000000 24.4421997070000003
Sn Ag O C H
7 1 18 1 1
Selective dynamics
Direct
0.1269399970000009 0.1786199960000019 0.2258799969999998 F F F
0.6269400119999986 0.1786199960000019 0.2258799969999998 F F F
0.6261786743018076 0.6802943836803920 0.3617652484405093 T T T
0.3769400119999986 0.6786199809999971 0.2258799969999998 F F F
0.8769400119999986 0.6786199809999971 0.2258799969999998 F F F
0.3741951296918185 0.1796159254931132 0.3682978006402498 T T T
0.8790451454566803 0.1793050162563197 0.3683461597226496 T T T
0.1260456149464602 0.6786550328453911 0.3724843686863236 T T T
0.1269399970000009 0.6786199809999971 0.1720000059999975 F F F
0.6269400119999986 0.6786199809999971 0.1720000059999975 F F F
0.1267096496170486 0.1779140202802837 0.3102183027168403 T T T
0.6266619623571688 0.1781286592635375 0.3109190020153935 T T T
0.1269399970000009 0.6786199809999971 0.2797699870000017 F F F
0.6269400119999986 0.6786199809999971 0.2797699870000017 F F F
0.1267315659645804 0.1840815423744214 0.4180945578726498 T T T
0.6265453436023100 0.1787274578165649 0.4194116621872080 T T T
0.3769400119999986 0.3720799979999967 0.2258799969999998 F F F
0.8769400119999986 0.3720799979999967 0.2258799969999998 F F F

0.3839479377548207 0.8671873028745958 0.3765107290660248 T T T
0.8685944446570737 0.8671086732194501 0.3758603028045882 T T T
0.3769400119999986 0.9851499800000028 0.2258799969999998 F F F
0.8769400119999986 0.9851499800000028 0.2258799969999998 F F F
0.3849765100922421 0.4916310379547110 0.3752212670689363 T T T
0.8673011197398038 0.4915450269707465 0.3753756818634209 T T T
0.1297957513073707 0.5110501422979300 0.4850764531503390 T T T
0.1121172237335136 0.8476827187904807 0.4806318919237735 T T T
0.1223609517262388 0.6689040653940289 0.4642919418536198 T T T
0.1121118363623524 0.8559478634192658 0.5213024567190454 T T T

Ag-SnO_2-OCHO:
1.00000000000000
6.5065999030999997 0.0000000000000000 0.0000000000000000
0.0000000000000000 6.8080000877000000 0.0000000000000000
0.0000000000000000 0.0000000000000000 24.4421997070000003
Sn Ag O C H
7 1 18 1 1
Selective dynamics
Direct
0.1269399970000009 0.1786199960000019 0.2258799969999998 F F F
0.6269400119999986 0.1786199960000019 0.2258799969999998 F F F
0.6276889851164819 0.6792348779569272 0.3644734807060335 T T T
0.3769400119999986 0.6786199809999971 0.2258799969999998 F F F
0.8769400119999986 0.6786199809999971 0.2258799969999998 F F F
0.3747014140945638 0.1790935154786336 0.3671461664248473 T T T
0.8831580274381707 0.1792920092804735 0.3686981384808543 T T T
0.1337646978719842 0.6788427506628082 0.3658959731713127 T T T
0.1269399970000009 0.6786199809999971 0.1720000059999975 F F F
0.6269400119999986 0.6786199809999971 0.1720000059999975 F F F
0.1244406297218441 0.1793802162800624 0.3100830388856273 T T T
0.6301962438924454 0.1791444807553135 0.3105206158667600 T T T
0.1269399970000009 0.6786199809999971 0.2797699870000017 F F F
0.6269400119999986 0.6786199809999971 0.2797699870000017 F F F
0.1320085900215077 0.1790857315280835 0.4194238499948723 T T T
0.6276149745812724 0.1789997474775779 0.4181527956319484 T T T
0.3769400119999986 0.3720799979999967 0.2258799969999998 F F F
0.8769400119999986 0.3720799979999967 0.2258799969999998 F F F
0.3792583927597661 0.8705570447436151 0.3602388041618565 T T T
0.8788287062786845 0.8662105105727416 0.3728517394802734 T T T
0.3769400119999986 0.9851499800000028 0.2258799969999998 F F F
0.8769400119999986 0.9851499800000028 0.2258799969999998 F F F
0.3795132174022782 0.4874287841984580 0.3600431029685013 T T T
0.8786178384245272 0.4919995744262350 0.3728498948782357 T T T
0.1990545967042835 0.6754296953046460 0.4538305362261030 T T T
0.5561057010925925 0.6763305789224461 0.4530148897705441 T T T
0.3787304225173552 0.6732931324177209 0.4746270336634644 T T T
0.3761948944777090 0.6673556678344827 0.5199315479492286 T T T

Ag-SnO_2-CO:
1.00000000000000
6.5065999030999997 0.0000000000000000 0.0000000000000000
0.0000000000000000 6.8080000877000000 0.0000000000000000
0.0000000000000000 0.0000000000000000 24.4421997070000003
Sn Ag O C
7 1 17 1
Selective dynamics

Direct

0.1269399970000009	0.1786199960000019	0.2258799969999998	F	F	F
0.6269400119999986	0.1786199960000019	0.2258799969999998	F	F	F
0.6269705428369748	0.6796412297168292	0.3633166463341969	T	T	T
0.3769400119999986	0.6786199809999971	0.2258799969999998	F	F	F
0.8769400119999986	0.6786199809999971	0.2258799969999998	F	F	F
0.3730407230990943	0.1797401934583878	0.3690444070816419	T	T	T
0.8798322515077073	0.1795861757005997	0.3691627803053985	T	T	T
0.1263313544131049	0.6796449697066276	0.3717529509454293	T	T	T
0.1269399970000009	0.6786199809999971	0.1720000059999975	F	F	F
0.6269400119999986	0.6786199809999971	0.1720000059999975	F	F	F
0.1265944180016825	0.1791167600153616	0.3109127261990021	T	T	T
0.6265360592101610	0.1795355224948921	0.3112159925113342	T	T	T
0.1269399970000009	0.6786199809999971	0.2797699870000017	F	F	F
0.6269400119999986	0.6786199809999971	0.2797699870000017	F	F	F
0.1268844334244479	0.1799964301360899	0.4204164675433648	T	T	T
0.6263176988958771	0.1793922011972130	0.4196665413909434	T	T	T
0.3769400119999986	0.3720799979999967	0.2258799969999998	F	F	F
0.8769400119999986	0.3720799979999967	0.2258799969999998	F	F	F
0.3784135181052735	0.8666543705242291	0.3747277376658463	T	T	T
0.8743850790838530	0.8670007109615406	0.3754637615422195	T	T	T
0.3769400119999986	0.9851499800000028	0.2258799969999998	F	F	F
0.8769400119999986	0.9851499800000028	0.2258799969999998	F	F	F
0.3784169981038390	0.4925035822646938	0.3747967555755469	T	T	T
0.8746479424928721	0.4922405278143660	0.3753447908499944	T	T	T
0.5515000771900971	0.6794605629298028	0.5147666817848553	T	T	T
0.5942890645014788	0.6782107328259317	0.4695883658795937	T	T	T

Ag-SnO_2-H:

1.00000000000000

6.5065999030999997	0.0000000000000000	0.0000000000000000
0.0000000000000000	6.8080000877000000	0.0000000000000000
0.0000000000000000	0.0000000000000000	24.4421997070000003

Sn	Ag	O	H
7	1	16	1

Selective dynamics

Direct

0.1269399970000009	0.1786199960000019	0.2258799969999998	F	F	F
0.6269400119999986	0.1786199960000019	0.2258799969999998	F	F	F
0.6269400119999986	0.6795236994948642	0.3672642270656611	T	T	T
0.3769400119999986	0.6786199809999971	0.2258799969999998	F	F	F
0.8769400119999986	0.6786199809999971	0.2258799969999998	F	F	F
0.3733162153034013	0.1793240810470863	0.3677051016306808	T	T	T
0.8805637486966053	0.1793240810470863	0.3677051016306808	T	T	T
0.1269399970000009	0.6792352654762339	0.3665247728556063	T	T	T
0.1269399970000009	0.6786199809999971	0.1720000059999975	F	F	F
0.6269400119999986	0.6786199809999971	0.1720000059999975	F	F	F
0.1269399970000009	0.1795909656560892	0.3101384907876261	T	T	T
0.6269400119999986	0.1791658825218790	0.3104670824916367	T	T	T
0.1269399970000009	0.6786199809999971	0.2797699870000017	F	F	F
0.6269400119999986	0.6786199809999971	0.2797699870000017	F	F	F
0.1269399970000009	0.1789982185110108	0.4198752268442233	T	T	T
0.6269400119999986	0.1789398023253030	0.4178620239235086	T	T	T
0.3769400119999986	0.3720799979999967	0.2258799969999998	F	F	F
0.8769400119999986	0.3720799979999967	0.2258799969999998	F	F	F
0.3689567096761097	0.8697192336744486	0.3679353322408982	T	T	T
0.8849232843238853	0.8697192336744486	0.3679353322408982	T	T	T
0.3769400119999986	0.9851499800000028	0.2258799969999998	F	F	F

0.8769400119999986	0.9851499800000028	0.2258799969999998	F	F	F
0.3691903149110651	0.4889749893880590	0.3685886563379603	T	T	T
0.8846896790889298	0.4889749893880590	0.3685886563379603	T	T	T
0.6269400119999986	0.6819601093890100	0.4391080952692366	T	T	T

Supporting Figures

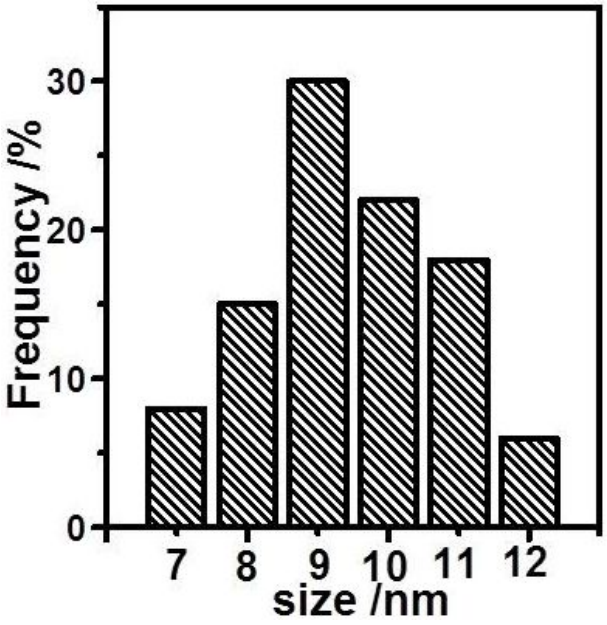

Figure S1. Particle size statistics of the core/shell Ag_{75}/(A-Sn(IV))$_{25}$.

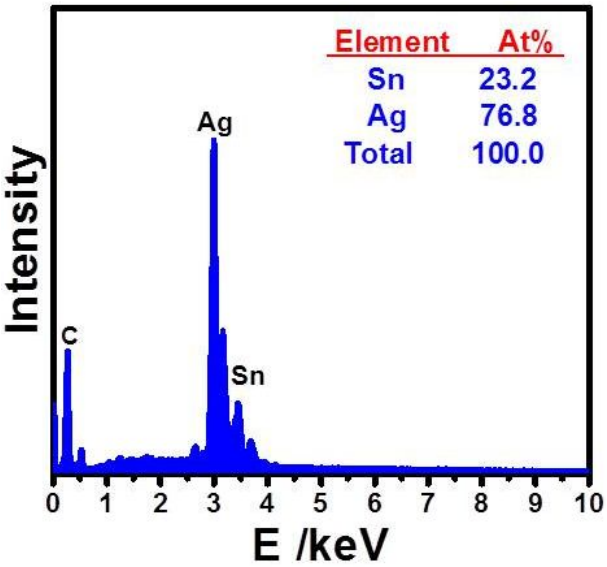

Figure S2. The SEM-EDS of Ag_{75}/(A-Sn(IV))$_{25}$.

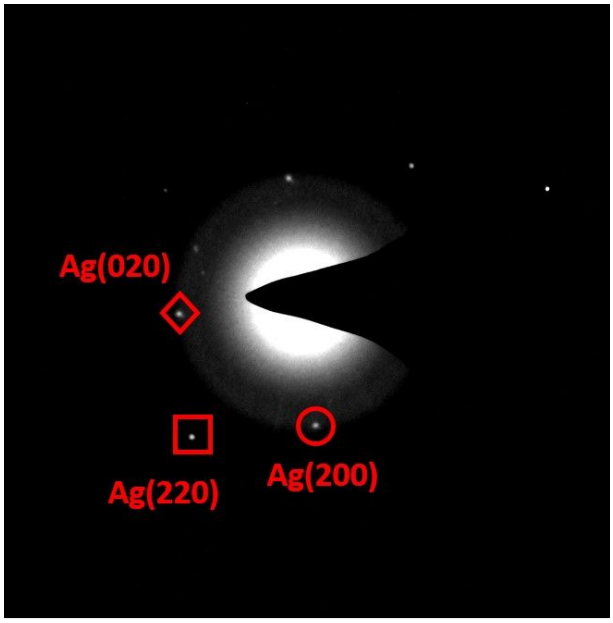

Figure S3. The selected area electron diffraction of $Ag_{75}/(A\text{-}Sn(IV))_{25}$.

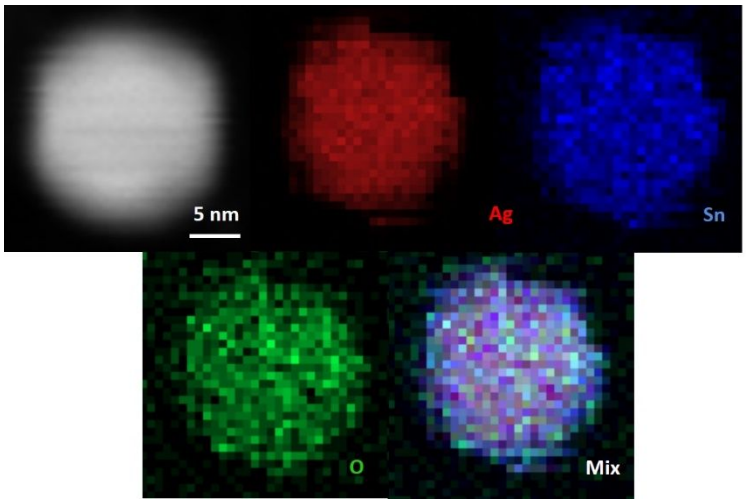

Figure S4. HAADF-STEM image and corresponding element mappings of $Ag_{75}/(A\text{-}Sn(IV))_{25}$.

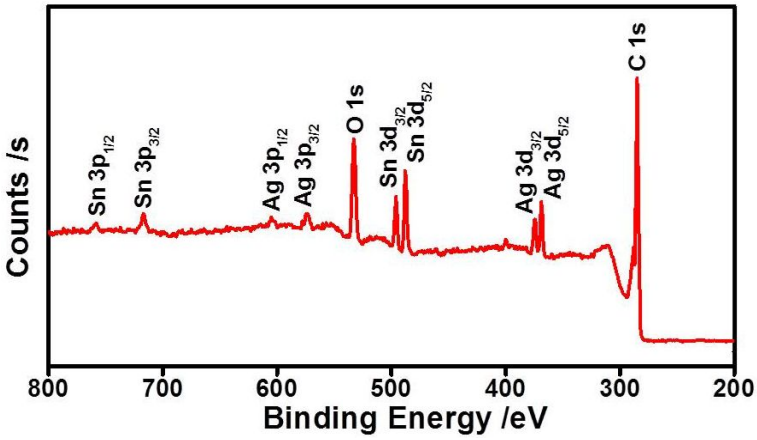

Figure S5. XPS spectrum of overall survey spectrum of $Ag_{75}/(A\text{-}Sn(IV))_{25}$.

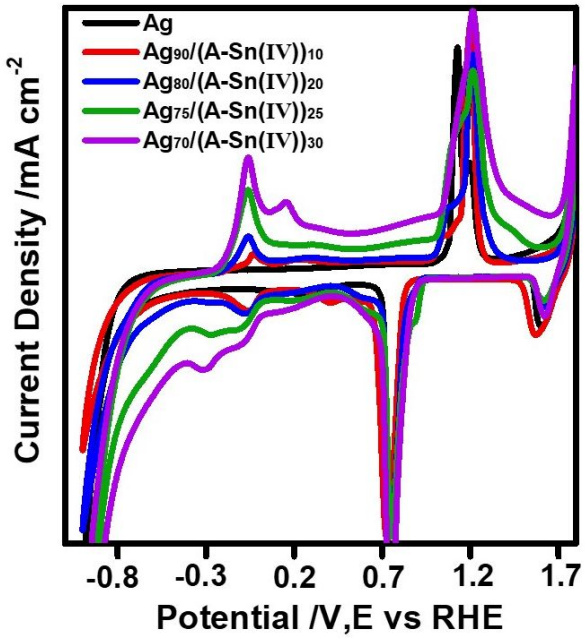

Figure S6. CV curves of Ag/(A-Sn(IV)) in Ar-saturated 0.5 M $NaHCO_3$ solution at a scan rate of 50 mV/s.

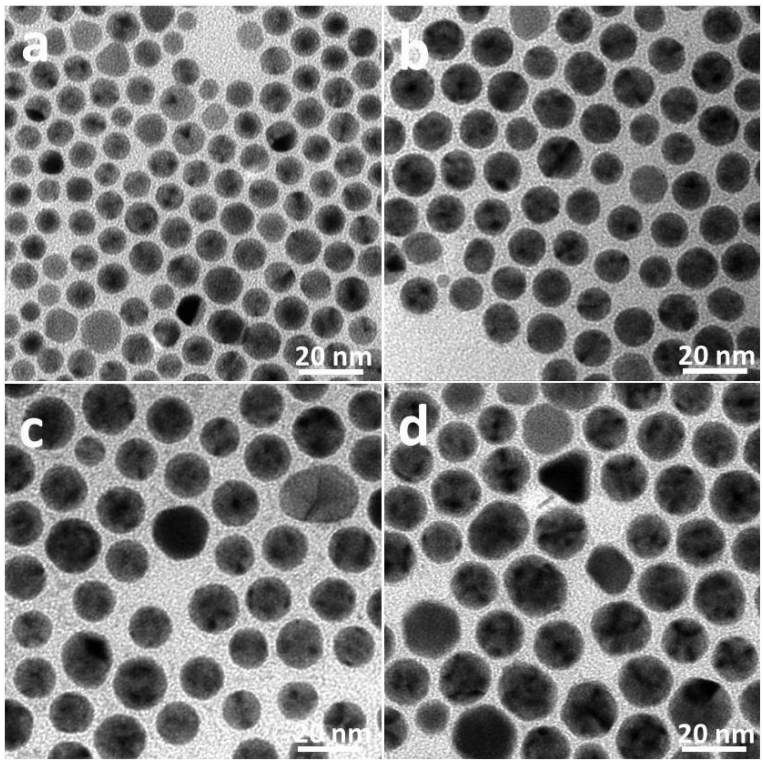

Figure S7. TEM images of (a) Ag, (b) Ag_{90}/(A-Sn(IV))$_{10}$, (c) Ag_{80}/(A-Sn(IV))$_{20}$, and (d) Ag_{70}/(A-Sn(IV))$_{30}$.

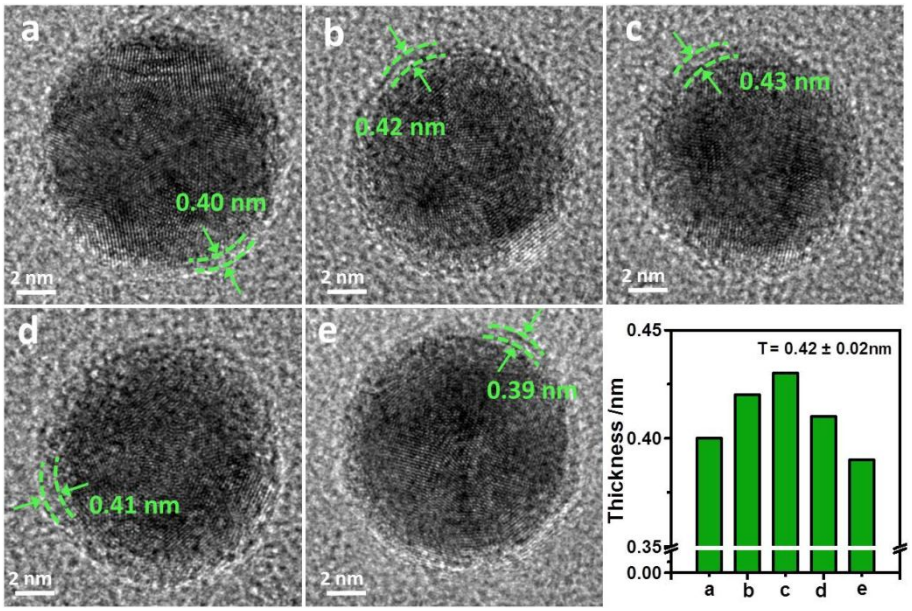

Figure S8. (a-e) HRTEM images and shell thickness statistics of $Ag_{90}/(A\text{-}Sn(IV))_{10}$.

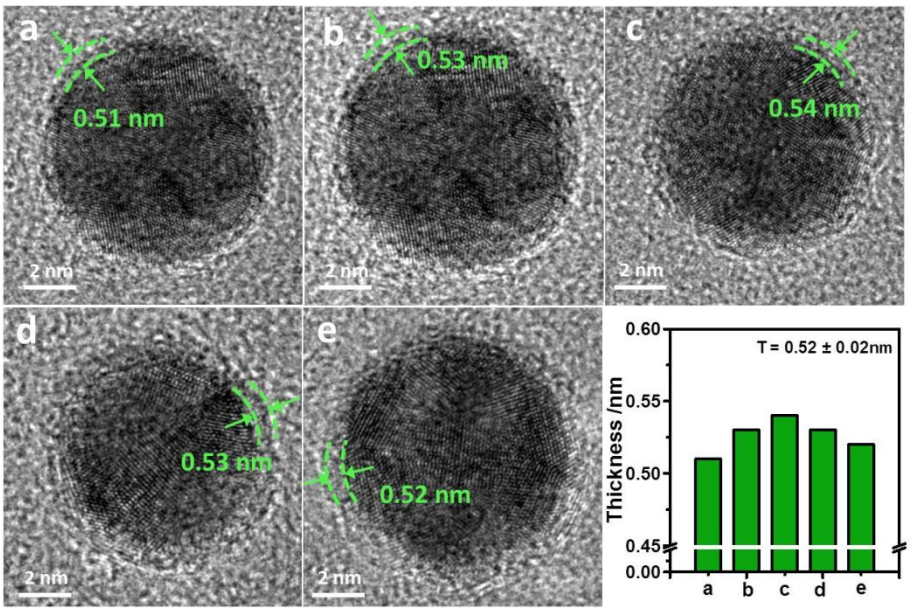

Figure S9. (a-e) HRTEM images and shell thickness statistics of $Ag_{80}/(A\text{-}Sn(IV))_{20}$.

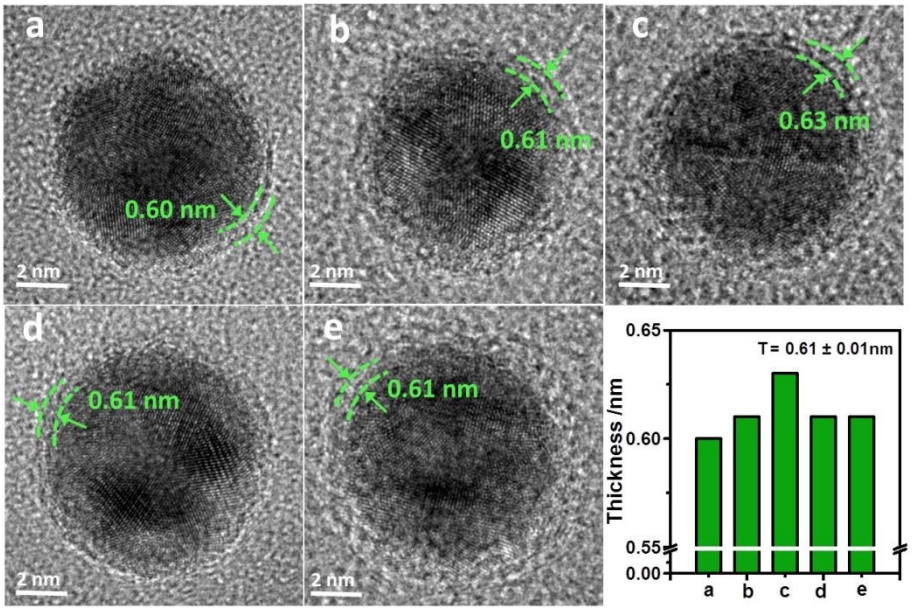

Figure S10. (a-e) HRTEM images and shell thickness statistics of $Ag_{75}/(A\text{-}Sn(IV))_{25}$.

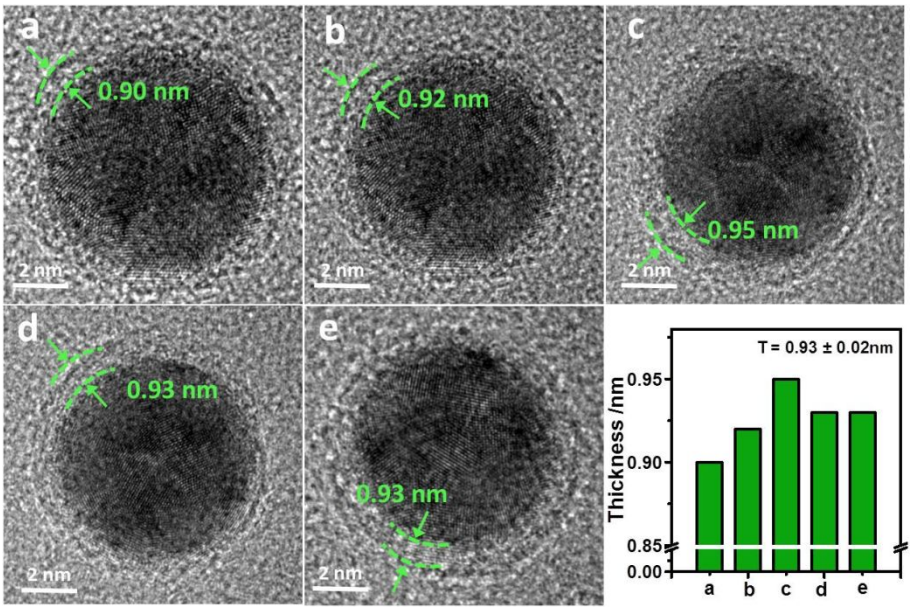

Figure S11. (a-e) HRTEM images and shell thickness statistics of $Ag_{70}/(A\text{-}Sn(IV))_{30}$.

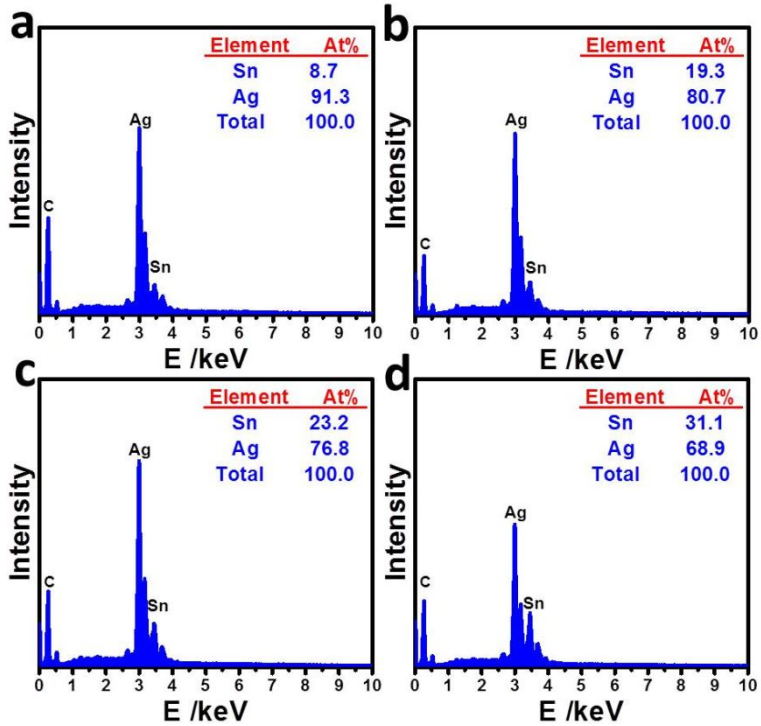

Figure S12. The SEM-EDS results of (a) $Ag_{90}/(A\text{-}Sn(IV))_{10}$, (b) $Ag_{80}/(A\text{-}Sn(IV))_{20}$, (c) $Ag_{75}/(A\text{-}Sn(IV))_{25}$, and (d) $Ag_{70}/(A\text{-}Sn(IV))_{30}$.

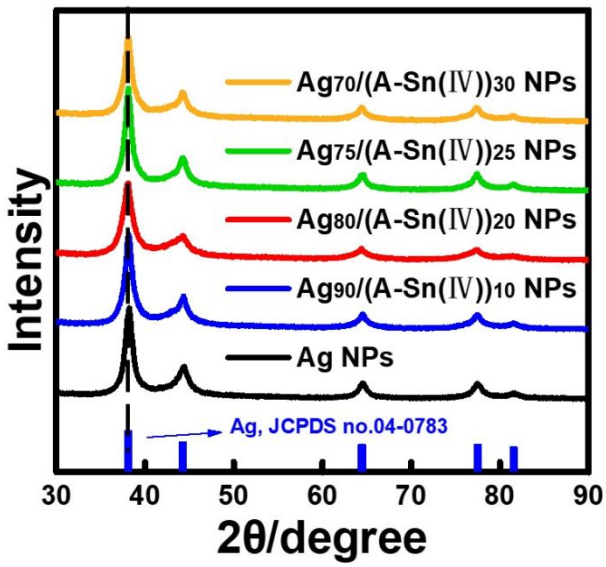

Figure S13. The XRD patterns of Ag NPs and four Ag/(A-Sn(IV)) catalysts.

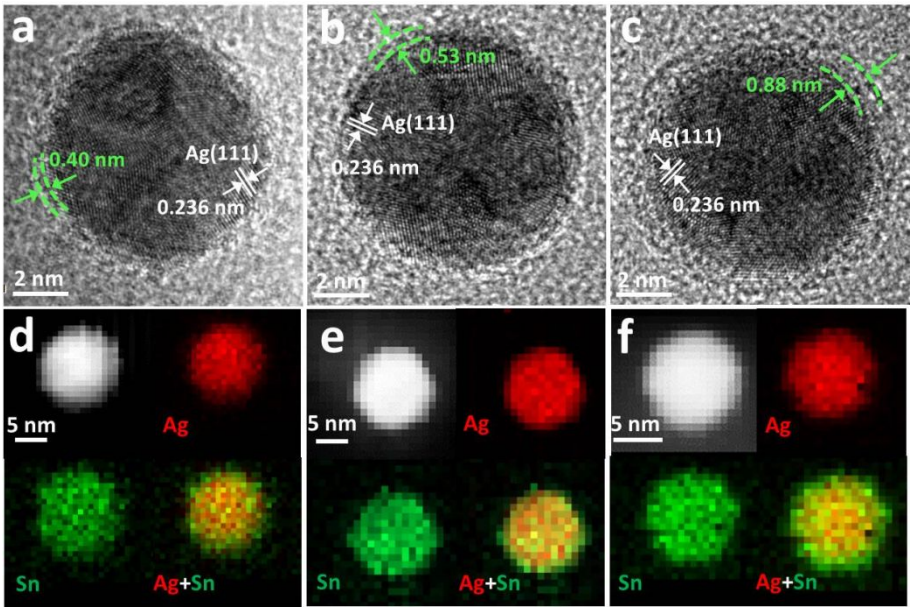

Figure S14. (a-c) HRTEM images, (d-f) HAADF-STEM images and corresponding element mappings of (a, d) core/shell Ag/(A-Sn(IV)) (Ag_{90}/(A-Sn(IV))$_{10}$, (b, e) Ag_{80}/(A-Sn(IV))$_{20}$, and (c, f) Ag_{70}/(A-Sn(IV))$_{30}$.

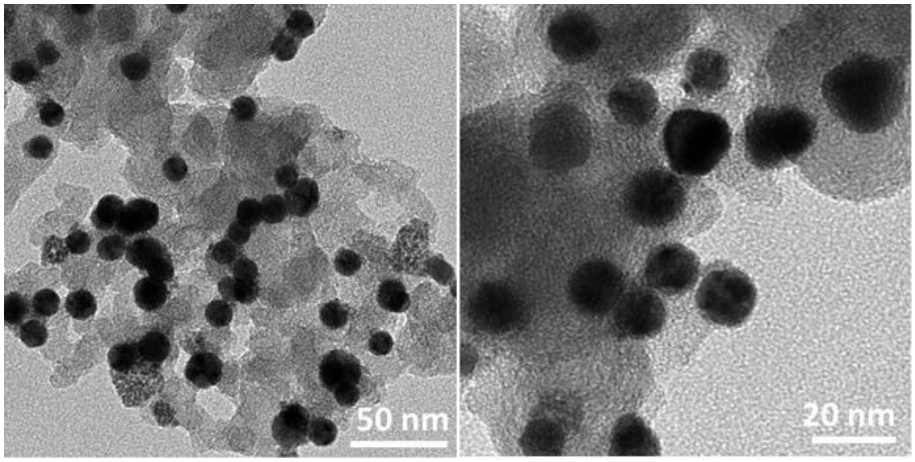

Figure S15. TEM images of Ag_{75}/(A-Sn(IV))$_{25}$/C.

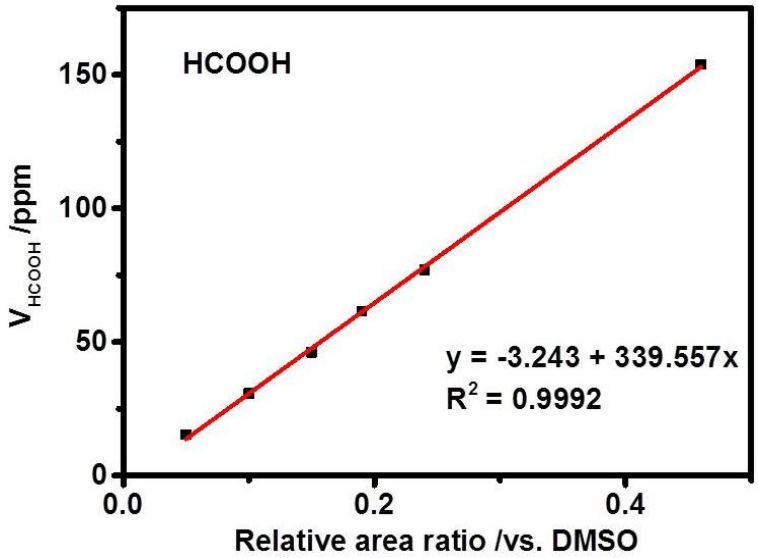

Figure S16. Linear relationship between the formic acid volume and relative area vs. DMSO. The linear correlation coefficient is 0.9992. The standard curve was made as follows: 1 mL aqueous formic acid with different concentrations (0.02 μL/mL, 0.04 μL/mL, 0.06 μL/mL, 0.08 μL/mL, 0.1 μL/mL, and 0.2 μL/mL) was mixed with 0.2 mL D_2O and 0.1 mL, 14.08 mM DMSO solution. DMSO solution was added as internal standard.

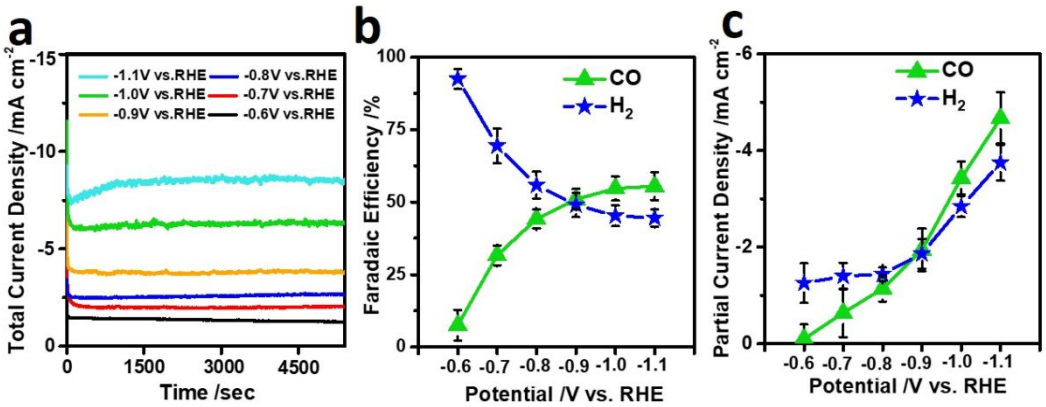

Figure S17. The electrochemical CO_2 reduction of (a) *i*-T curves, (b) faradaic efficiencies, and (c) partial current densities at different applied voltages for Ag.

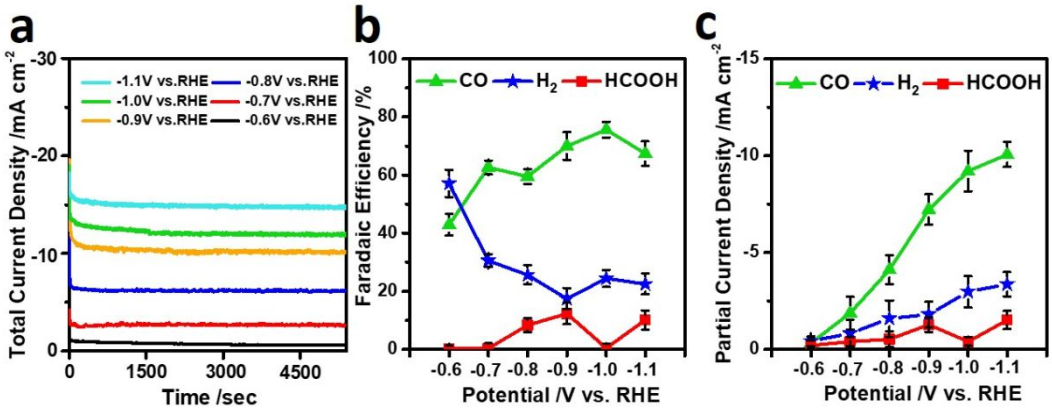

Figure S18. The electrochemical CO_2 reduction of (a) *i*-T curves, (b) faradaic efficiencies, and (c) partial current densities at different applied voltages for Ag_{90}/(A-Sn(IV))$_{10}$.

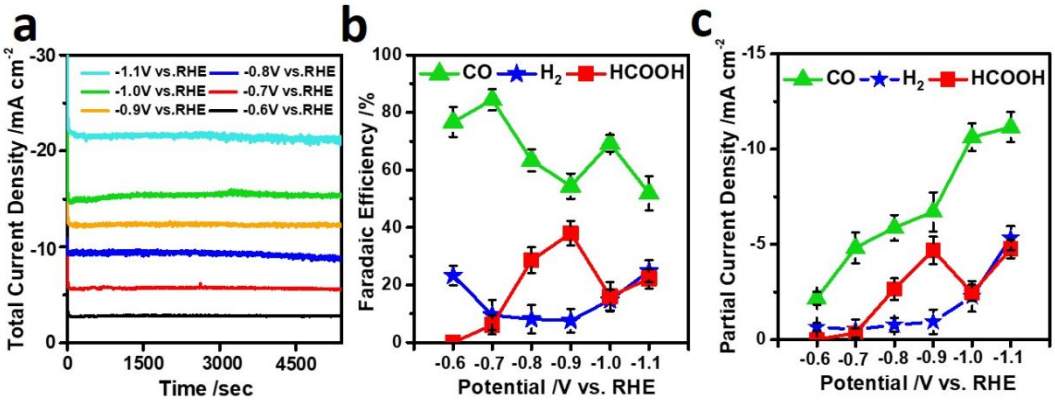

Figure S19. The electrochemical CO_2 reduction of (a) *i*-T curves, (b) faradaic efficiencies, and (c) partial current densities at different applied voltages for Ag_{80}/(A-Sn(IV))$_{20}$.

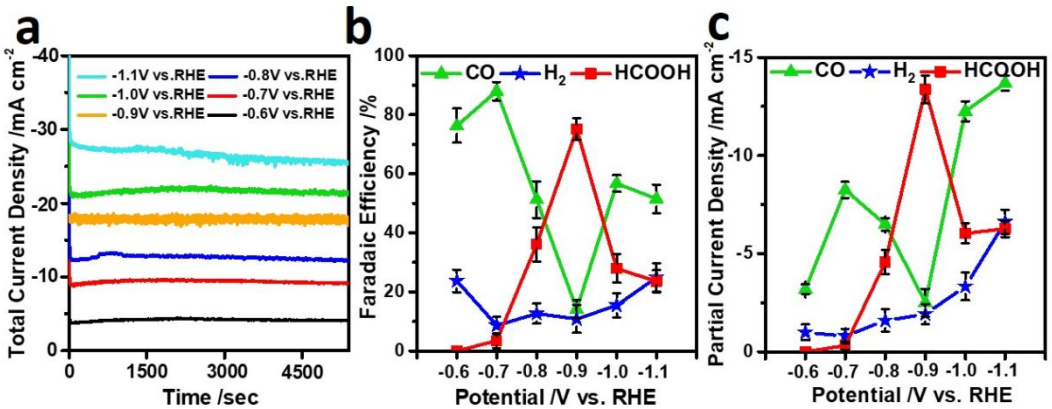

Figure S20. The electrochemical CO_2 reduction of (a) *i*-T curves, (b) faradaic efficiencies, and (c) partial current densities at different applied voltages for $Ag_{75}/(A\text{-}Sn(IV))_{25}$.

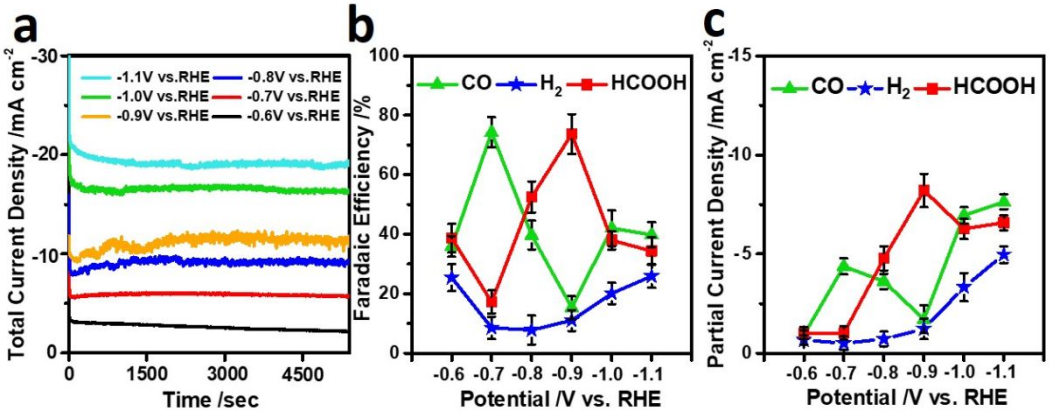

Figure S21. The electrochemical CO_2 reduction of (a) *i*-T curves, (b) faradaic efficiencies, and (c) partial current densities at different applied voltages for $Ag_{70}/(A\text{-}Sn(IV))_{30}$.

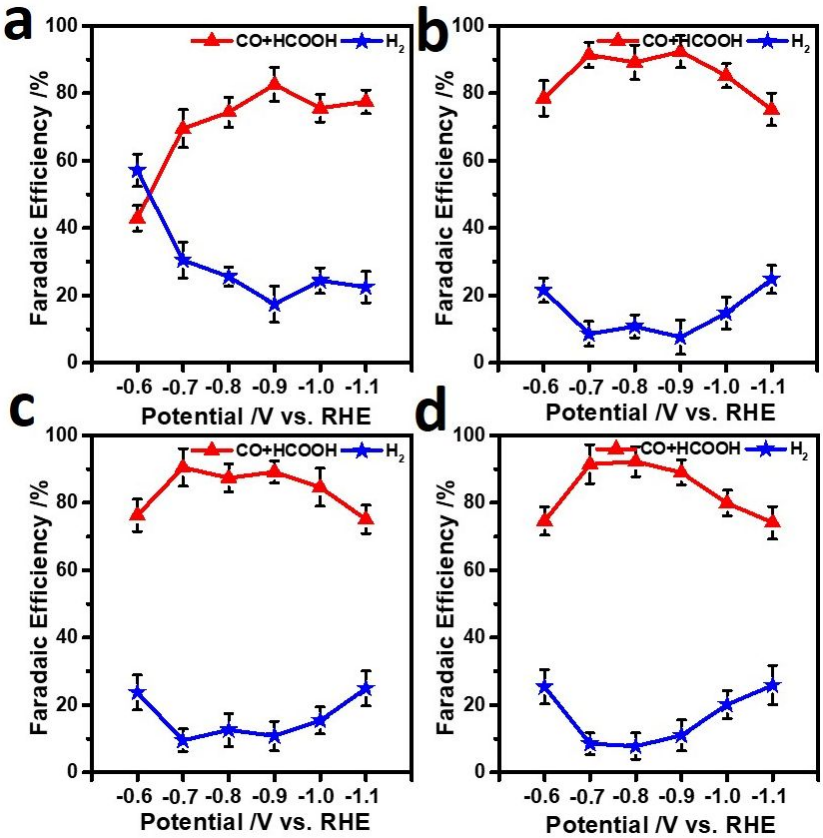

Figure S22. The electrochemical CO_2 reduction faradaic efficiencies of (a) $Ag_{90}/(A\text{-}Sn(IV))_{10}$, (b) $Ag_{80}/(A\text{-}Sn(IV))_{20}$, (c) $Ag_{75}/(A\text{-}Sn(IV))_{25}$, and (d) $Ag_{70}/(A\text{-}Sn(IV))_{30}$.

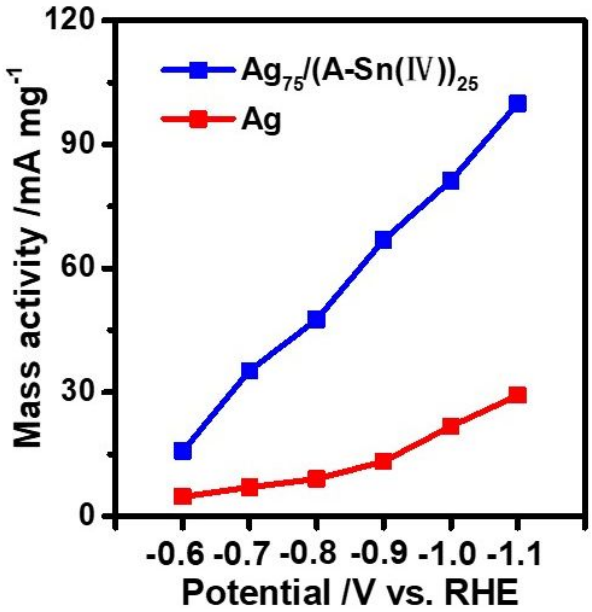

Figure S23. The mass activities of $Ag_{75}/(A\text{-}Sn(IV))_{25}$ and Ag for electrochemical CO_2 reduction.

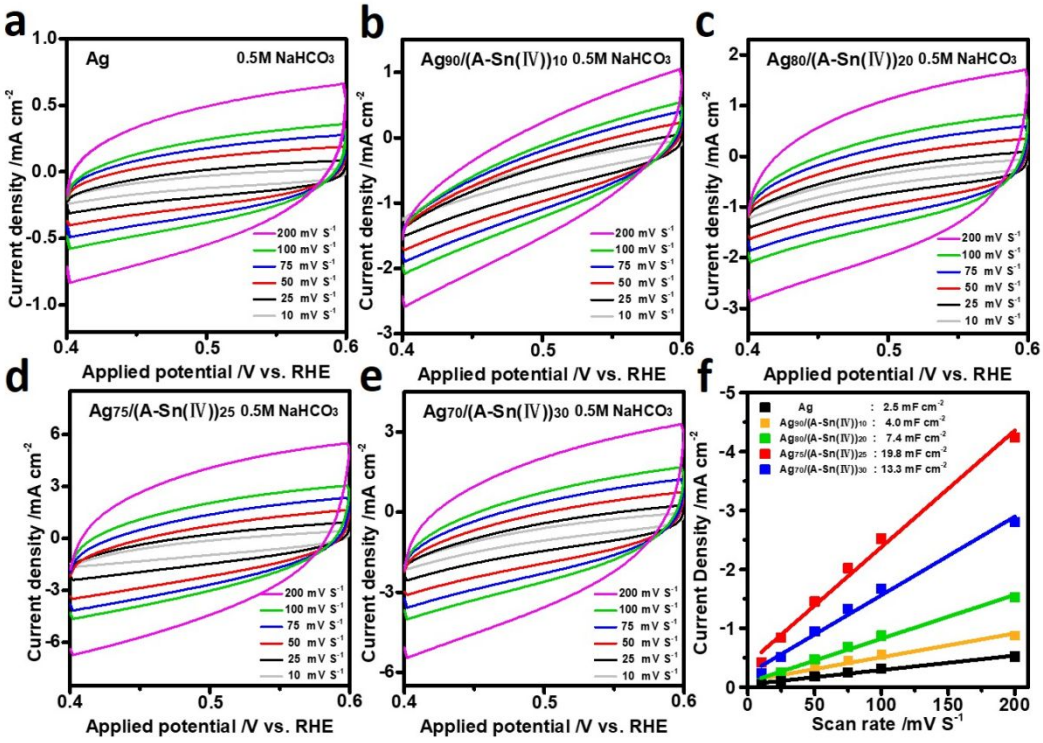

Figure S24. CV curves of (a) Ag, (b) $Ag_{90}/(A\text{-}Sn(IV))_{10}$, (c) $Ag_{80}/(A\text{-}Sn(IV))_{20}$, (d) $Ag_{75}/(A\text{-}Sn(IV))_{25}$ and (e) $Ag_{70}/(A\text{-}Sn(IV))_{30}$ catalysts with various scan rates. (f) The electric double layer capacitance value of different catalysts.

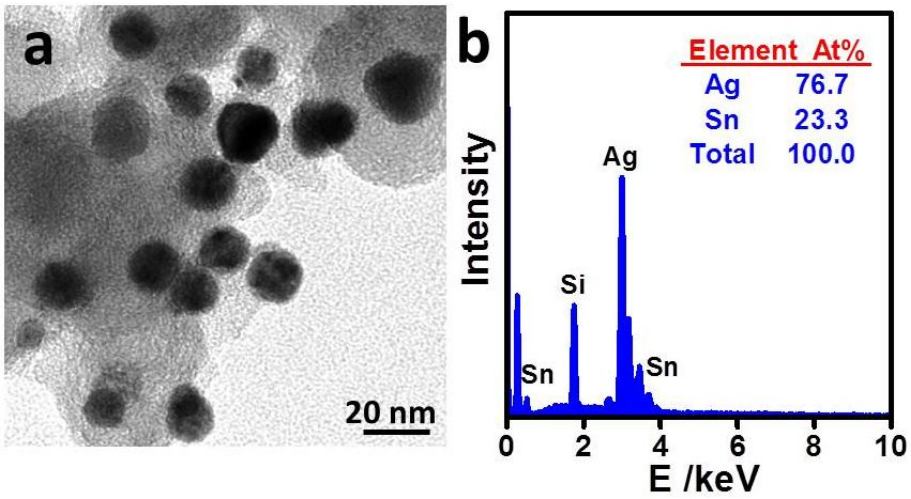

Figure S25. (a) TEM image and (b) SEM-EDS pattern of Ag_{75}/(A-Sn(IV))$_{25}$ after stability test.

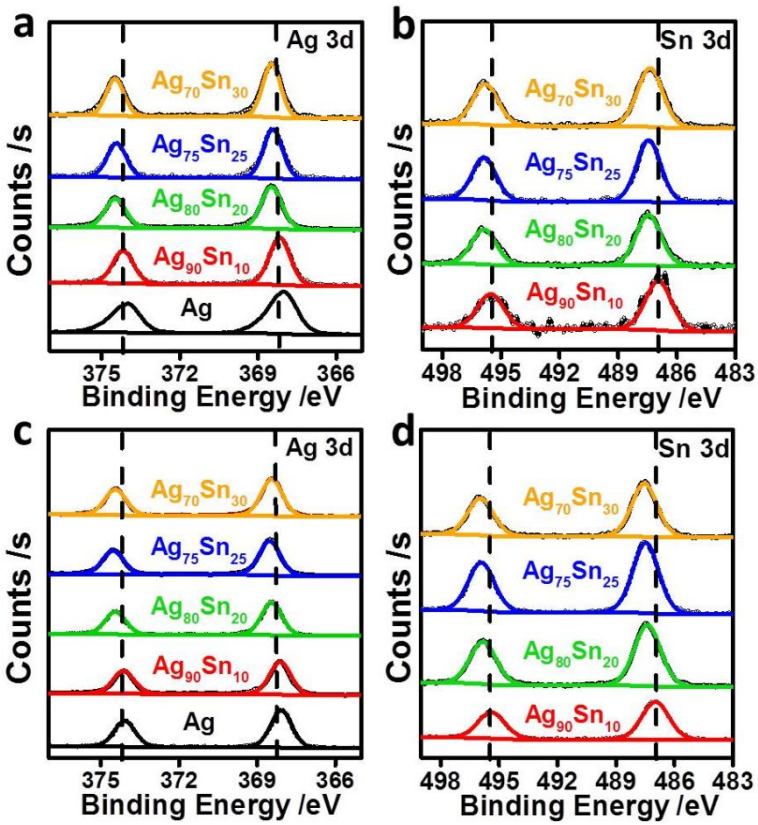

Figure S26. XPS spectra of the core/shell Ag/(A-Sn(IV)) (a, b)before and (c, d) after the electrochemical reduction reaction.

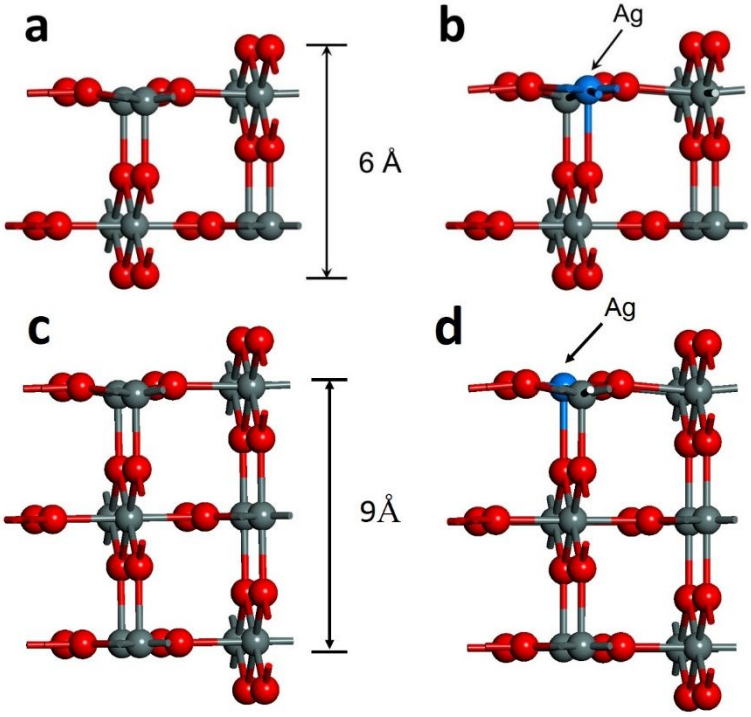

Figure S27. Geometry model of (a) 6Å pure SnO_2 (110) surface, (b) 6Å Ag/SnO_2 (110) surface, (c) 9Å pure SnO_2 (110) surface and (d) 9Å Ag/SnO_2 (110) surface with one Ag atom substituting Sn atom on the surface. Sn, O and Ag atoms are presented by dark grey, red and blue spheres, respectively.

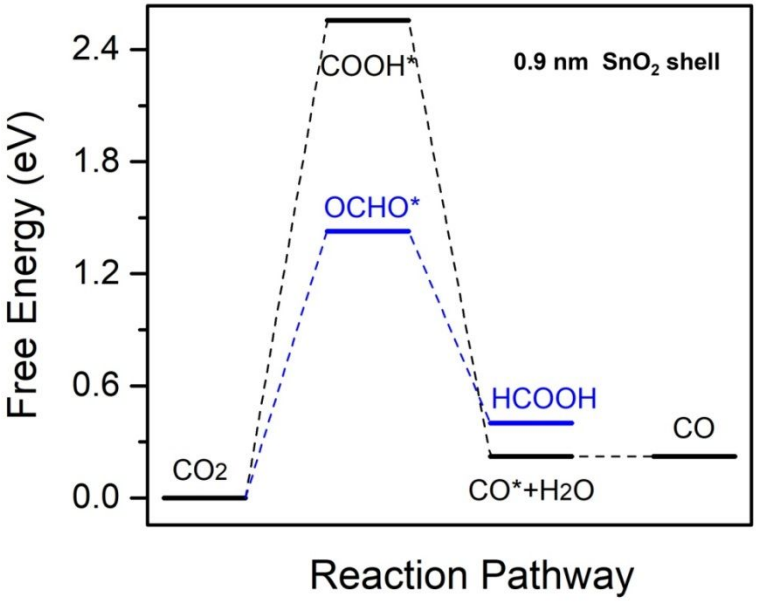

Figure S28. Free energy profiles of two ECR pathways on 0.9 nm SnO_2 shell.

Table S1. The ECR data of Ag/(A-Sn(IV)) NPs catalysts.

Catalyst	Potential [a] (V vs.RHE)	Product					
		CO		HCOOH		H_2	
		FE [b] (%)	Partial C·D [c] (mA cm^{-2})	FE (%)	Partial C·D (mA cm^{-2})	FE (%)	Partial C·D (mA cm^{-2})
Ag	-0.6	7.5	0.10	-	-	90.1	1.20
	-0.7	**29.5**	**0.64**	**-**	**-**	**67.4**	**1.40**
	-0.8	41.2	1.08	-	-	55.4	1.42
	-0.9	**50.1**	**1.91**	**-**	**-**	**48.1**	**1.84**
	-1.0	52.7	3.34	-	-	46.3	2.71
	-1.1	54.5	4.49	-	-	41.5	3.38
Ag_{90}/(A-Sn(IV))$_{10}$	-0.6	42.4	0.31	-	-	56.5	0.39
	-0.7	**68.5**	**1.87**	**-**	**-**	**29.5**	**0.82**
	-0.8	64.3	4.04	7.1	0.47	22.8	1.48
	-0.9	**68.1**	**7.19**	**11.3**	**1.22**	**14.7**	**1.51**
	-1.0	75.3	9.19	-	-	22.7	2.77
	-1.1	65.9	10.01	9.4	1.41	20.6	3.12
Ag_{80}/(A-Sn(IV))$_{20}$	-0.6	74.1	2.07	-	-	22.7	0.63
	-0.7	**83.4**	**4.82**	**5.1**	**0.35**	**7.3**	**0.54**
	-0.8	63.8	5.82	27.6	2.58	8.1	0.77
	-0.9	**53.4**	**6.67**	**35.7**	**4.60**	**7.6**	**0.94**
	-1.0	69.2	10.62	15.4	2.41	10.8	2.07
	-1.1	48.1	10.89	20.5	4.79	21.7	5.33
Ag_{75}/(A-Sn(IV))$_{25}$	-0.6	72.7	3.11	-	-	20.7	0.76
	-0.7	**88.0**	**8.25**	**6.4**	**0.45**	**6.6**	**0.51**
	-0.8	50.7	6.45	34.7	4.44	12.4	1.59
	-0.9	**9.8**	**1.51**	**75.1**	**13.36**	**10.1**	**1.92**
	-1.0	53.2	11.95	22.4	5.89	10.7	3.18
	-1.1	50.5	13.69	21.4	6.12	22.0	6.54
Ag_{70}/(A-Sn(IV))$_{30}$	-0.6	31.4	0.88	36.2	0.97	23.1	0.55
	-0.7	**73.1**	**4.38**	**14.9**	**1.01**	**7.2**	**0.50**
	-0.8	37.9	3.54	52.5	4.78	7.1	0.67
	-0.9	**13.9**	**1.62**	**71.7**	**8.11**	**10.7**	**1.21**
	-1.0	41.2	6.89	35.1	6.08	19.7	3.21
	-1.1	37.2	7.41	32.4	6.31	21.7	4.52

Where potential [a] means applied voltage, FE [b] means faradaic efficiency, and partial C·D [c] means partial current density.

Table S2. Zero-pint energy correction (E_{ZPE}), entropy contribution (TS), and the total free energy correction ($G - E_{elec}$) in this study.

Species	E_{ZPE} (eV)	$\int CpdT$ (eV)	$-TS$ (eV)	$G - E_{elec}$ (eV)
H_2	0.27	0.09	–0.42	–0.06
H_2O	0.57	0.10	–0.69	–0.02
CO	0.13	0.09	–0.61	–0.39
CO_2	0.31	0.12	–0.68	–0.25
HCOOH	0.89	0.09	–0.99	–0.01
COOH* on Ag/(A-Sn(IV))	0.61	0.11	–0.26	0.46
HCOO* on Ag/(A-Sn(IV))	0.62	0.09	–0.18	0.53
CO* on Ag/(A-Sn(IV))	0.17	0.09	–0.23	0.03
H* on Ag/(A-Sn(IV))	0.19	0.01	–0.01	0.19
COOH* on SnO_2 (110)	0.60	0.11	–0.26	0.45
HCOO* on SnO_2 (110)	0.63	0.09	–0.16	0.56
CO* on SnO_2 (110)	0.18	0.09	–0.23	0.03
COOH* on Ag(111)	0.58	0.12	–0.30	0.40
CO* on Ag(111)	0.16	0.10	–0.28	–0.02
H* on Ag(111)	0.13	0.01	–0.02	0.12

Table S3. Comparison of different catalysts for electrochemical reduction of CO_2 to C_1 product.

	Catalyst	Electrolyte	Potential (V vs.RHE)	Loading Mass (mg cm^{-2})	Main Product FE	Current Density (mA cm^{-2})	Ref.
	Ag_{75}/(A-Sn(IV))$_{25}$	0.5 M $NaHCO_3$	-0.7	0.45	CO (88%)	9.4	This Work
	Ag_{75}/(A-Sn(IV))$_{25}$	0.5 M $NaHCO_3$	-0.9	0.45	HCOOH (75.1%)	17.8	This Work
Ag		0.1 M $KHCO_3$	-1.35	N/A	CO (40%)	10.0	[1]
	Tri-Ag-NPs	0.1 M $KHCO_3$	-0.856	0.637	CO (96.8%)	1.25	[2]
	CoO_x	0.1 M Na_2SO_4	-0.25	0.07	HCOOH (90%)	9.0	[3]
	Sn-graphene	0.1 M	-1.16	0.05	HCOOH	21.1	[4]

	$NaHCO_3$			(89%)		
SnO2/graphene	0.1 M $NaHCO_3$	-1.16	0.05	HCOOH (93.6%)	10.2	[5]
Sn/SnO_x	0.5 M $NaHCO_3$	-0.7	N/A	HCOOH (58%)	2.5	[6]
Sn on gas diffusion electrode	0.5 M $NaHCO_3$	-1.10	2.6	C_1 FE (82%)	8.13	[7]
Core-shell Ag-Sn	0.5 M $NaHCO_3$	-0.80	1	C_1 FE (90%)	19.5	[8]
Nanoscale Sn/SnO_2	0.1 M $NaHCO_3$	-1.26	0.2	C_1 FE (86.2%)	9	[9]
Bi nanosheet	0.5 M $NaHCO_3$	-1.5 (vs.SCE)	1	HCOOH (>95%)	16	[10]
C-Cu/SnO_2-0.8	0.5 M $KHCO_3$	-0.7	13.5	CO (93%)	4.6	[11]
C-Cu/SnO_2-1.8	0.5 M $KHCO_3$	-0.9	14.3	HCOOH (95%)	N/A	[11]
Sn	0.5 M $KHCO_3$	-1.8 (vs.SCE)	N/A	HCOOH (40.2%)	12.0 A/cm^2	[12]
Sn particles	0.5M $KHCO_3$+ 0.5 M KCl	-1.4	0.1	HCOOH (64.6%)	90	[13]

References

1. Hatsukade, T.; Kuhl, K. P.; Cave, E. R.; Abram, D. N.; Jaramillo, T. F., Insights Into The Electrocatalytic Reduction of CO_2 on Metallic Silver Surfaces, *Phys. Chem. Chem. Phys.* **2014**, *16*, 13814-13819.
2. Liu, S.; Tao, H.; Zeng, L.; Liu, Q.; Xu, Z.; Liu, Q.; Luo, J. L., Shape-Dependent Electrocatalytic Reduction of CO_2 to CO on Triangular Silver Nanoplates, *J. Am. Chem. Soc.* **2017**, *139*, 2160-2163.
3. Gao, S.; Lin, Y.; Jiao, X.; Sun, Y.; Luo, Q.; Zhang, W.; Li, D.; Yang, J.; Xie, Y., Partially Oxidized Atomic Cobalt Layers For Carbon Dioxide Electroreduction to Liquid Fuel, *Nature* **2016**, *529*, 68-71.
4. Hori, Y.; Wakebe, H.; Tsukamoto, T.; Koga, O., Electrocatalytic Process of CO Selectivity in Electrochemical Reduction of CO_2 at Metal Electrodes in Aqueous Media, *Electrochim. Acta* **1994**, *39*, 1833-1839.
5. Zhang, S.; Kang, P.; Meyer, T. J., Nanostructured Tin Catalysts for Selective Electrochemical

Reduction of Carbon Dioxide to Formate, *J. Am. Chem. Soc.* **2014**, *136*, 1734-1737.

6. Chen, Y.; Kanan, M. W., Tin Oxide Dependence of the CO_2 Reduction Efficiency on Tin Electrodes and Enhanced Activity for Tin/Tin Oxide Thin-Film Catalysts, *J. Am. Chem. Soc.* **2012**, *134*, 1986-1989.
7. Irtem, E.; Andreu, T.; Parra, A.; Hernandez-Alonso, M. D.; Garcia-Rodriguez, S.; Riesco-Garcia, J. M.; Penelas-Perez, G.; Morante, J. R., Low-Energy Formate Production From CO_2 Electroreduction Using Electrodeposited Tin on GDE, *J. Mater. Chem. A* **2016**, *4*, 13582-13588.
8. Luc, W.; Collins, C.; Wang, S.; Xin, H.; He, K.; Kang, Y.; Jiao, F., Ag-Sn Bimetallic Catalyst with a Core–Shell Structure for CO_2 Reduction, *J. Am. Chem. Soc.* **2017**, *139*, 1885-1893.
9. Zhang, S.; Kang, P.; Meyer, T. J., Nanostructured Tin Catalysts for Selective Electrochemical Reduction of Carbon Dioxide to Formate, *J. Am. Chem. Soc.* **2014**, *136*, 1734-1737.
10. Han, N.; Wang, Y.; Yang, H.; Deng, J.; Wu, J.; Li, Y.; Li, Y., Ultrathin Bismuth Nanosheets From in Situ Topotactic Transformation For Selective Electrocatalytic CO_2 Reduction to Formate, *Nat. Commun.* **2018**, *9*, 1320-1327.
11. Li, Q.; Fu, J.; Zhu, W.; Chen, Z.; Shen, B.; Wu, L.; Xi, Z.; Wang, T.; Lu, G.; Zhu, J. J.; Sun, S., Tuning Sn-Catalysis for Electrochemical Reduction of CO_2 to CO via the Core/Shell Cu/SnO_2 Structure, *J. Am. Chem. Soc.* **2017**, *139*, 4290-4293.
12. Jiang, H.; Zhao, Y.; Wang, L.; Kong, Y.; Li, F.; Li, P., Electrochemical CO_2 Reduction to Formate on Tin Cathode: Influence of Anode Materials, *J. CO_2 Util.* **2018**, *26*, 408-414.
13. Del Castillo, A.; Alvarez-Guerra, M.; Solla-Gullón, J.; Sáez, A.; Montiel, V.; Irabien, A., Electrocatalytic Reduction of CO_2 to Formate Using Particulate Sn Electrodes: Effect of Metal Loading and Particle Size, *Appl. Energy* **2015**, *157*, 165-173.